IV International Conference on Particle-based Methods – Fundamentals and Applications
PARTICLES 2015
E. Oñate, M. Bischoff, D.R.J. Owen, P. Wriggers & T. Zohdi (Eds)

# INVESTIGATION OF GREEN WATER IN FPSO BY A PARTICLE-BASED NUMERICAL OFFSHORE TANK

**CEZAR AUGUSTO BELLEZI[1 3] *, DAVI TEODORO FERNANDES[1 3], LIANG-YEE CHENG[2 3], MÁRCIO MICHIHARU TSUKAMOTO[2 3], KAZUO NISHIMOTO[1 3]**

[1]Department of Naval and Ocean Engineering
Escola Politécnica of University of São Paulo
Av. Prof. Mello Moraes, 2231, São Paulo – SP, Brasil
e-mail: polinaval@usp.br, web page : http://www.pnv.poli.usp.br

[2]Department of Construction Engineering
Escola Politécnica of University of São Paulo
Av. Prof. Almeida Prado, 83, São Paulo – SP, Brasil
web page: http://www.pcc.usp.br

[3]Numerical Offshore Tank (TPN)
Av. Prof. Mello Moraes, 2231, São Paulo – SP, Brasil
web page: http://www.tpn.usp.br

*cbellezi@tpn.usp.br

**Key words:** Green water, hydrodynamic impact, MPS method, large scale simulation

**Abstract.** The green water is a highly non linear hydrodynamic phenomenon that occurs when the wave height exceeds the freeboard of the floating structures in harsh environments, and may compromise the operation and security of the on deck equipment. In the present study, in order to assess the effects of the green water phenomenon in FPSO and FLNG systems, the Moving Particle Semi-implicit (MPS) method, which is a fully lagrangian particle-method for incompressible flow, is adopted to model the complex fluid structure interaction problem. This article is focused on the recent developments of the MPS based simulation system of Numerical Offshore Tank (TPN-USP) and its application to the real scale offshore engineering problem. Results of large scale simulations using distributed memory architecture for models from 30 million to 100 million particles are presented.

## 1 INTRODUCTION

The importance of offshore oil and gas exploitation in deepwater and ultra deepwater increased significantly along the past decade. The deepwater oil production grows from less than 2% of the worldwide oil production in 2000 to more than 10% ten years later. The oil exploration in deepwater and ultra deepwater is performed by floating offshore structures . In severe weather conditions, dangerous hydrodynamic impact phenomena related to large incoming waves may occur and may compromise the operation and safety of the floating structures.

One of the hydrodynamic impact phenomena related to the violent waves impact is the green water. The green water occurs when the sea surface height surpasses the freeboard of the floating structures due to the relative motion between the structure and the sea surface, resulting in water boarding on deck. In case of floating production, storage and offloading (FPSO) platforms, the water that invades the deck may damage the equipment of the production plant. The green water is a highly nonlinear hydrodynamic impact phenomenon very challenging to numerical modeling. The complexity of the phenomenon is related to strong fluid-structure interaction with violent impulsive loads on structures with a variety of geometries and large free surface deformation and fragmentation due to wave breaking and splashing.

In order to study the complex green water phenomenon on FPSO, Moving Particle Semi-Implicit (MPS) method is adopted in the present study. The MPS method was developed by Koshizuka et al. [1] and Koshizuka & Oka [2] to model the incompressible flow based on a fully lagrangian scheme in which the computational domain is entirely modeled as particles. The method models very well problems involving large free surface deformations, fragmentation and merging, as well as complex shaped, moving and deformable structures.

The MPS method was applied to the green water investigation by Shibata & Koshizuka [3] and Shibata et al. [4] and Shibata et al. [5]. The validation of green water phenomenon for the MPS-based system developed at TPN-USP is presented by Bellezi et al. [6] based on the comparison between the numerical results with the experimental data obtained by Lee et al. [7]. Bellezi et al. [8] study the effect of the bow shaped in the green water phenomenon for fixed model under head seas.

The main disadvantage of the particle method is its large demand to computational resources, which limits the size and the resolution of the models. To overcome this challenge, particle based simulation systems using domain decomposition and distributed memory techniques were developed [9] [10].

The focus of the present paper is to show the evolvements of a particle-based modeling of the numerical offshore tank for the investigation of the green water, from the low resolution fixed reduced scale models to the simulation of large real scale floating models up to 100 million particles. The results presented in this work are divided in three parts: The first part shows the effects of the model resolution through the comparison of the results of a low resolution model with 1.6 million particle and a higher resolution model with 12 million particles . The second part shows the simulation of the 100 million particle model based on the Lee et al. [7] experiments and the performance of the distributed memory computation is brief analyzed. Finally, in the third part, a practical engineering application for a real scale model platform is carried out considering a large FLNG platform at critical weather conditions at Santos Basin.

## 2 NUMERICAL METHOD

The Moving Particle Semi-Implicit (MPS) method, also called Moving Particle Simulation, is a fully lagrangian particle-based CFD method for the incompressible free surface flow.

### 2.1 Governing equations

The governing equations solved by the MPS method are the continuity equation (eq. 1) and the Navier Stokes equation (eq. 2).

$$\frac{D\rho}{Dt} = -\rho(\nabla.\vec{u}) = 0 \tag{1}$$

$$\frac{D\vec{u}}{Dt} = -\frac{1}{\rho}\nabla P + \vartheta\nabla^2\vec{u} + \frac{\vec{f}}{\rho} + \vec{g} \tag{2}$$

where $\rho$ is the fluid density, $\vartheta$ is the fluid kinematic viscosity, $P$ the pressure, $\vec{g}$ the gravity acceleration, $\vec{f}$ any other given field force and $\vec{u}$ the velocity of a given particle.

The viscous term of the Navier Stokes equation is neglected in the studies carried out herein because the phenomena involving violent wave impact are often related to gravitational forces and high Reynold numbers.

### 2.2 Numerical model

The formulation of the MPS method is based on a weight function $\omega(r)$ given by.

$$\omega(r) = \begin{cases} \frac{r_e}{r} - 1\, for\ (0 \le r < r_e) \\ 0\, for\ (r_e \le r) \end{cases} , \tag{3}$$

where, $r_e$ is a neighborhood radius and $r = |\vec{r_i} - \vec{r_j}|$ is the distance between two given particles $i$ and $j$.

An important parameter is the particle number density (*pnd*). It is given by:

$$[pnd]_i = \sum_{j\neq i} \omega(|\vec{r_j} - \vec{r_i}|) \quad . \tag{4}$$

The algebraic operators of the MPS method are derived based on the weighted contribution of the neighbor particles. The gradient operator for a given $\Phi$ scalar quantity is presented by the eq. 5. The laplacian operator for a $\Phi$ scalar quantity is given by the eq. 6.

$$[\nabla\Phi]_i = \frac{d}{pnd^0}\sum_{j\neq i}\left[\frac{(\Phi_j - \Phi_i)}{|\vec{r_j} - \vec{r_i}|^2}(\vec{r_j} - \vec{r_i})\omega(|\vec{r_j} - \vec{r_i}|)\right] \tag{5}$$

$$[\nabla^2\Phi]_i = \frac{2d}{pnd^0\delta}\sum_{j\neq i}[(\Phi_j - \Phi_i)\omega(|\vec{r_j} - \vec{r_i}|)] \quad , \tag{6}$$

where $pnd^0$ is the particle number density of regarding to initial particle configuration of a particle with fulfilled neighborhood, $d$ is the dimension of the problem (2 for two dimensional modeling and 3 for three dimensional problems). The parameter $\delta$ is calculated based on the initial particle configuration and is given by

$$\delta = \frac{\int_V \omega(r)r^2 dv}{\int_V \omega(r) dv} \tag{7}$$

### 2.3 Algorithm

The algorithm of the MPS method is presented in Figure 1.

The algorithm is divided into two main steps. The first step is the explicit calculation to estimate velocity, position and particle number density of all fluid particles based on Eq. (2), except the pressure gradient term. In the second step, a linear system of Poisson equations of pressure (eq. 8) is solved to satisfy the mass conservation.

$$[\nabla^2 P^{n+1}]_i = -k\frac{\rho}{\Delta t^2}\frac{[pnd^*]_i - pnd^0}{pnd^0} \quad , \tag{8}$$

where $pnd^*$ is the particle number density calculated in the explicit step. The $pnd^0$ is the initial particle number density and $\Delta t$ is the time step. $k$ is the pressure smooth coefficient.

From the pressures obtained implicitly, the pressure gradient is calculated and the velocity and the position of the fluid particles are corrected.

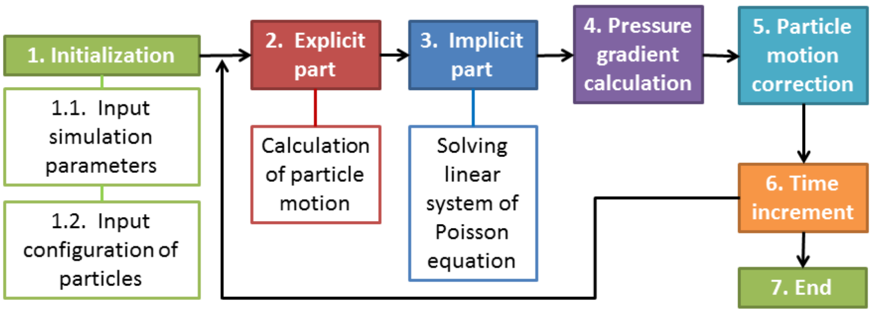


**Figure 1:** MPS method algorithm

## 2.4 Free surface boundary condition

The free surface boundary condition proposed by Lee et al. [11] is adopted in this study.

$$[pnd^*]_i = \beta \cdot pnd^0 \tag{9}$$

$$[N^*]_i = \gamma \cdot N^0 \tag{10}$$

where $N$ is the number of particles inside the neighborhood radius for a given particle and $N^0$ the reference number of particles in the neighborhood, considering a particle whose neighborhood is completely fulfilled in the initial configuration. Based on Lee et al. [11] results, the coefficients are $\beta = 0.97$ and $\gamma = 0.85$.

## 2.5 Free solid modeling

In the MPS method the entire domain is modeled as particles, including the solid surface. The solid surface is modeled with three rows of particles. The row of solid particles in contact with the fluid are modeled as wall particles. The other two rows consist of dummy particles. The dummy particles are used to assure the correct calculation of the particle number density of the wall particles.

For the numerical offshore tank modeling, three types of solid are considered: fixed solid, solid with forced motion and a free floating solid. The velocity of the fixed and the forced motion solids are imposed as Dirichlet boundary conditions. On the other hand, the motion of the free floating solid are calculated based on forces and moments obtained from the integration of the pressure on the solid surface. The center of gravity, the mass and the moment of inertia of each free floating solid are input parameters.

This implementation of the free floating solid is based on Sueyoshi et al. [12] and Sueyoshi et al. [13] work. Test and validation of the free floating solid implementation used in the present work are presented by Tsukamoto et al. [14] and Tsukamoto et al. [15].

## 3 FPSO NUMERICAL SIMULATION

In the present study the development of the particle-based numerical offshore tank for the investigation of green water phenomena are illustrated in three parts. The first is the validation through the comparison between the experimental data of Lee et al. [7] and the numerical results for a low resolution model of Bellezi et al. [6] with 1.6 million particles, and the numerical result of a higher resolution model, with 12 million particles, obtained by using the distributed memory framework for parallel processing developed by Fernandes [9]. The objective of this first stage is to show how the increase of the model resolution, which was limited in the previous works by hardware restrictions, could improve the results.

The second part consists of the simulation of a floating model with 100 million particles and the analysis is focused on the processing performance of the distributed memory version of MPS-TPN simulation system. Finally, the third part shows a practical engineering application using a very high resolution model to investigate the green water phenomenon in head seas on a FLNG system under Santos Basin extreme wave conditions.

### 3.1 Numerical towing tank

In the present work, the green water occurrences were investigated using a model inside a numerical towing tank as shown in Figure 2.

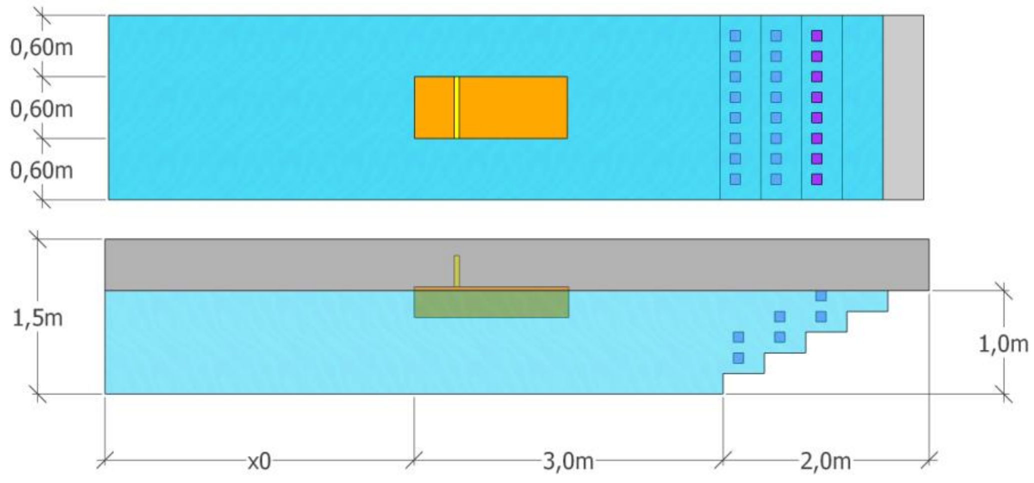


**Figure 2:** Main dimensions of the numerical tank

The waves were generated by a piston type wavemaker positioned in the left end of the tank. The piston type wavemaker was modeled as a forced solid wall with sinusoidal horizontal translation motion. A stair shaped beach and small fixed boxes were placed at the right end of the tank to absorb the waves and the disturbances due the body wave diffraction. The lateral walls of the tank were modeled as fixed ones. The distance between the model side and the tank lateral wall are equal to the beam of the model.

The waves conditions used in the sections 3.2 and 3.3 are based on those used by Lee et al.

[7] and presented in Table 1. After the wave calibration, the distance between the model and wavemaker ($x_0$) was obtained. The determination of this distance is necessary due the numerical damping that reduces the wave amplitude along the tank. More details about the wave calibration are presented in Bellezi et al. [6].

**Table 1:** Wave parameters

| Wave Condition | Amplitude | Wave length | Wavemaker period | Wavemaker amplitude | Distance between wavemaker and model ($x_o$) |
|---|---|---|---|---|---|
| 1 | 4.500 cm | 225 cm | 1.28 s | 0.04 m | 2.2 m |
| 2 | 5.625 cm | 225 cm | 1.28 s | 0.05 m | 2.2 m |
| 3 | 6.750 cm | 225 cm | 1.28 s | 0.06 m | 2.2 m |
| 4 | 6.000 cm | 300 cm | 1.39 s | 0.05 m | 2.2 m |
| 5 | 7.500 cm | 300 cm | 1.39 s | 0.06 m | 2.0 m |
| 6 | 9.000 cm | 300 cm | 1.39 s | 0.08 m | 2.7 m |
| 7 | 7.500 cm | 375 cm | 1.55 s | 0.07 m | 3.1 m |
| 8 | 9.375 cm | 375 cm | 1.55 s | 0.08 m | 2.7 m |
| 9 | 11.250 cm | 375 cm | 1.55 s | 0.10 m | 3.0 m |

## 3.2 Validation and convergence analysis by fixed model

This section is focused on the validation of the particle based method for the simulation of green water phenomenon. The numerical results are compared to the experimental ones obtained by Lee et al. [7], which used a reduced scale fixed model in head seas condition. The model geometry and the position of the pressure probes are presented in Figure 3.

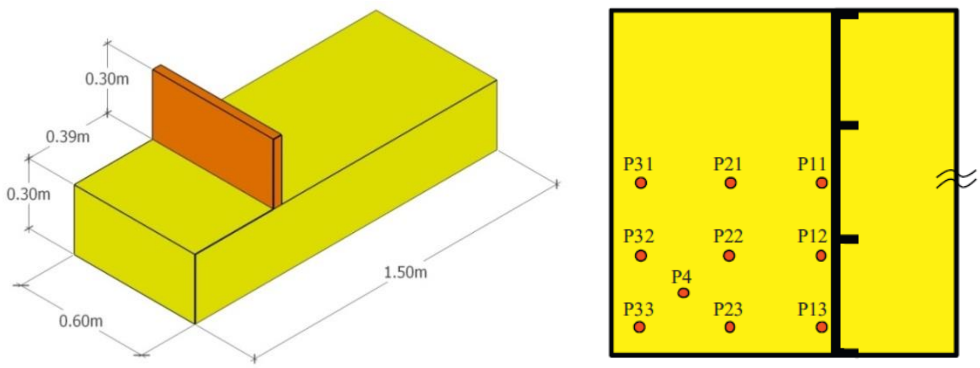


(a) (b)

**Figure 3:** Model main dimensions (a) and position of pressure probes on deck (b)

In Bellezi et al. [6] the resulted obtained by a low resolution model, with 1.6 million particle, were compared to the experimental measurements. In the present work, taking the advantage of a new version of the simulation system for distributed memory architecture, a higher resolution model, of which the distance between particles is half of those used in the previous work, is used. The numerical parameters for the simulations using the low and higher resolution models are given in Table 2.

The Figure 4 shows the pressure histories at the P11 pressure probe. Figure 4-a shows the unfiltered pressure time series, and Figure 4-b shows filtered data by local mean value.

**Table 2:** Numerical parameters of the simulations

| | **Coarse resolution model** | **High resolution model** |
|---|---|---|
| **Distance between particles [m]** | 0.02 | 0.01 |
| **Time step [s]** | 0.001 | 0.0005 |
| **Number of particles** | ≈1,600,000 | ≈12,000,000 |
| **Simulation time [s]** | 20 | 20 |
| **Subdomains** | 1 | 10 |
| **Pressure smooth coefficient** | 0.075 | 0.05 |

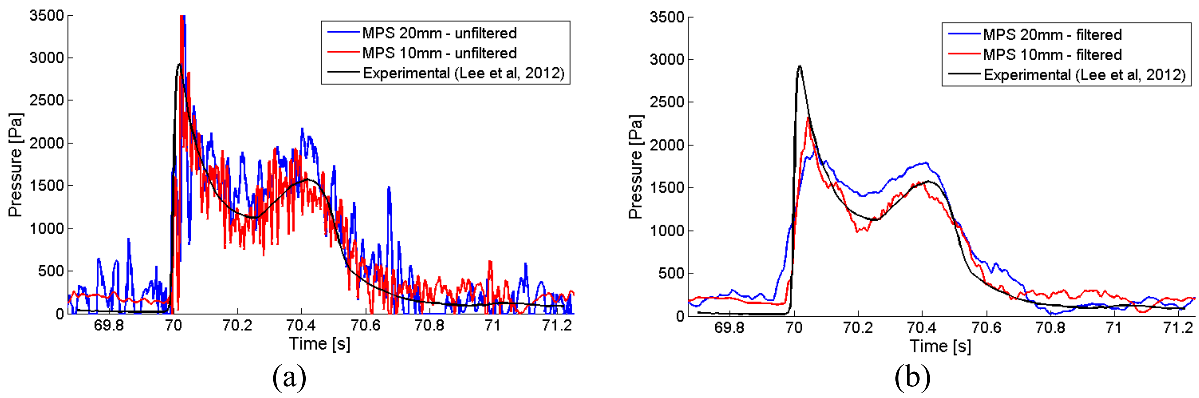


**Figure 4:** Pressure at P11 pressure probe for wave 9 –unfiltered (a) and filtered (b) numerical results

The P11 pressure probe is located in the center of the deck in front of the vertical bulkhead of the model. It registers the highest pressures of all the pressure probes located at the deck. The pressures histories shown in Figure 4 present two peaks pattern typical of wave impact load: The first peak is result of the merging of the water that come from the bow and from both sides during the ingress phase; The second peak is associated to the collapse of water column that occurs in the drainage phase of the green water phenomenon. Despite the oscillations of the computed pressure in P11, as the magnitude of the oscillations is lower than the magnitude of the peak pressure, in general the behavior of the numerical simulation matches the behavior of the experimental data. .

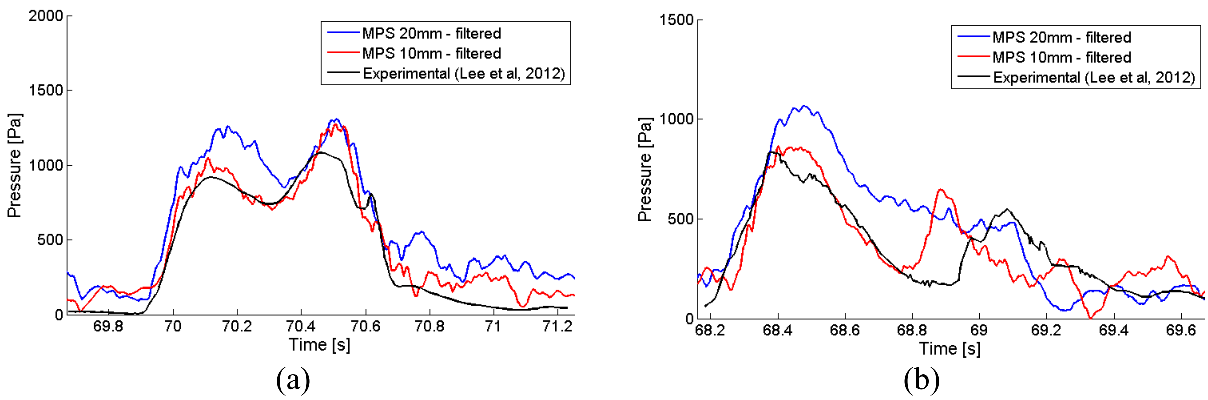


**Figure 5:** Filtered pressure at P21 (a) and P31 (b)

On the other hand, for the pressure probes in regions where lower pressures are registered, such as P21 and P31, the pressure oscillation magnitude gets closer to those of the pressure peaks. P21 and P31 have a lower embarking water level in relation to P11. The filtered results for the P21 and P31 region are presented at the Figure 5.

The result presented at Figure 4-b shows relatively small differences between the filtered results at P11 using the coarse or the finer resolution and both the results fit well with the experimental curve. However, for the pressure computed at P21 and P31, as shown in Figure 5, the behavior of the curve for the finer resolution is better than the coarse one. At P21 (Figure 5-a), the two peaks observed for the coarse resolution have almost the same value. On the other and, the first peak is significantly lower than the second peak for the finer resolution, which agrees well to the measurement. For P33, which involves even lower hydrodynamic pressures than P21, the coarse model is unable to show the occurrence of the two peaks, while the higher resolution model reproduced well the experimental result.

The simulation results showed that the coarse model predicts satisfactory the hydrodynamic impact at the most critical point, where the highest impact pressure occurs. However, for other regions where the level of embarking water is relatively low, the pressure oscillation magnitude is close to the magnitude of the pressure peaks and the higher resolution model is required for accurate assessment of the hydrodynamic loads.

### 3.3 Analysis of distributed memory parallel processing performance using a very high resolution free floating model

In this section simulations of the dynamic behavior of a free floating model with 100 million particles in total, including the towing tank, were carried out using the distributed memory architecture [9]. The reduced scale model used in the previous section was adopted. Wave condition 9 shown in Table 1 was considered in this section. The numerical parameters used in the simulation are presented in Table 3.

**Table 3:** Simulation numerical parameters

| | |
|---|---|
| **Distance between particles [m]** | 0.005 |
| **Time step [s]** | 0.00025 |
| **Number of particles** | ≈100,000,000 |
| **Simulation time [s]** | 10 |
| **Pressure smooth coefficient** | 0.045 |

The properties of the floating model are presented at Table 4.

**Table 4:** Properties of the floating model

| | |
|---|---|
| **Mass [kg]** | 229.5 |
| **Vertical center of gravity [m] (from kell)** | 0.196 |
| **Pitch moment of inertia [kg.m²]** | 30.83 |

The performance of the parallel processing by the distributed memory architecture were analyzed through a high resolution model with 100 million particles partitioned in 5 to 40 subdomains. Each subdomain was allocated to a node of computer cluster composed by 20 core AMD Shanghai of 2.66 GHz processors with 128GB of shared memory. When 40 subdomains are used, the 10 second simulation required around 250 hours of processing time.

Figure 6 provides some snapshots of the simulation of the low resolution model with 1.6 million particles, whose distance between particles is 0.02 meters, and the snapshots obtained using a very high resolution model with 100 million particles, whose distance between particles is 0.005 meters.

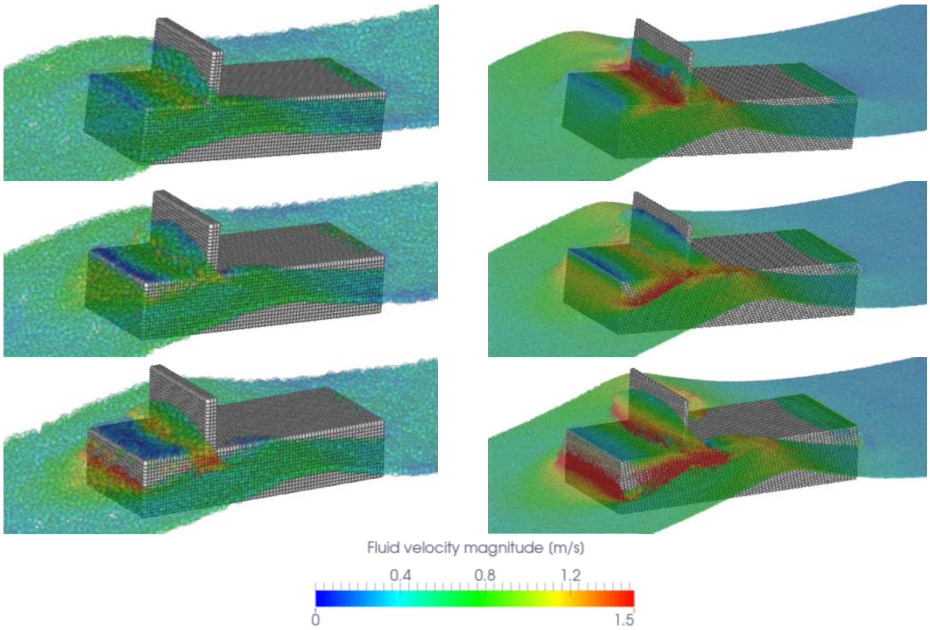


**Figure 6:** Snapshots of particle-based simulation of the floating models: Low resolution model with1.6 million particles (left) and very high resolution model with 100 million particles (right)

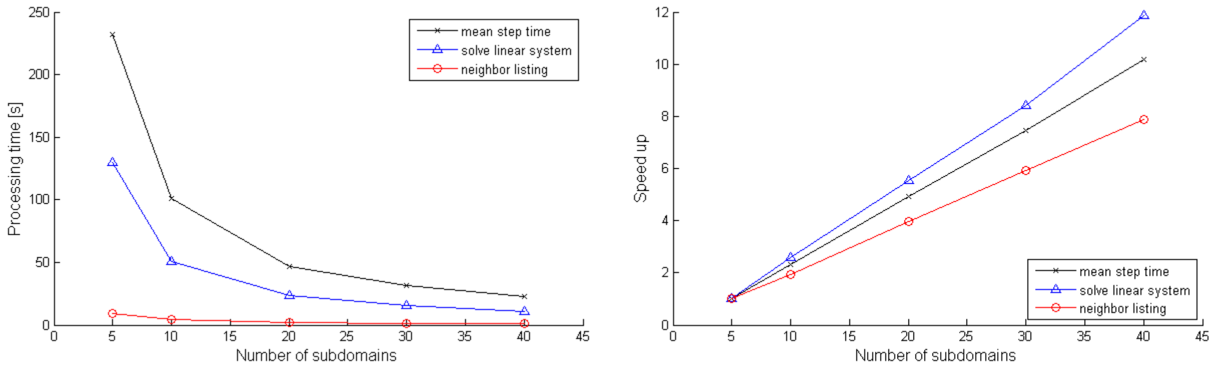


(a) (b)

**Figure 7:** Processing time (a) and speedup (b) in relation to the number of subdomains

Figure 7-a shows the effect of the increasing in the number of subdomains on the processing time. The processing time of the two most time consuming parts of the algorithm, the solution of the linear system and the neighborhood particle search, are also shown. Figure 7-a shows the speedup in relation to the time consumed for the 5 subdomain model. From the results, when 40 subdomains are used, the processing time required is nearly 10 times lower, showing relatively good speed up in this case.

### 3.4 Real scale model simulations

This section briefly presents results of the application of the particle-based numerical offshore tank to a practical engineering problem. It consists of a study on the green water occurrence of a FLNG system for the oil and gas exploitation in Santo Basin, Brazil.

The mooring system of the FLNG consists in a turret positioned at the bow, so the floating structure could align itself with the most severe weather condition direction. Thus, the FLNG system will operate aligned in head seas for the most severe weather condition, and the particle-based simulations were carried out for head seas of the maximum wave height for the century wave of the worst weather condition of the Santos Basin. The simulations were also carried out for the average, the maximum and the minimum operational draught of the system.

The particle model used in this analysis, including the numerical offshore tank, has around 30 million particles, and it is enough to describe the geometry of the vessel topside. The wave condition has approximately 20 seconds of period and the simulation of 200 seconds requires around 36 hours using 10 subdomains. Figure 8 presents some snapshots of the particle-based simulations. In the left column the sequence of the images shows the FLNG motion in wave for the maximum draught and in the right column for the minimum operational draught.

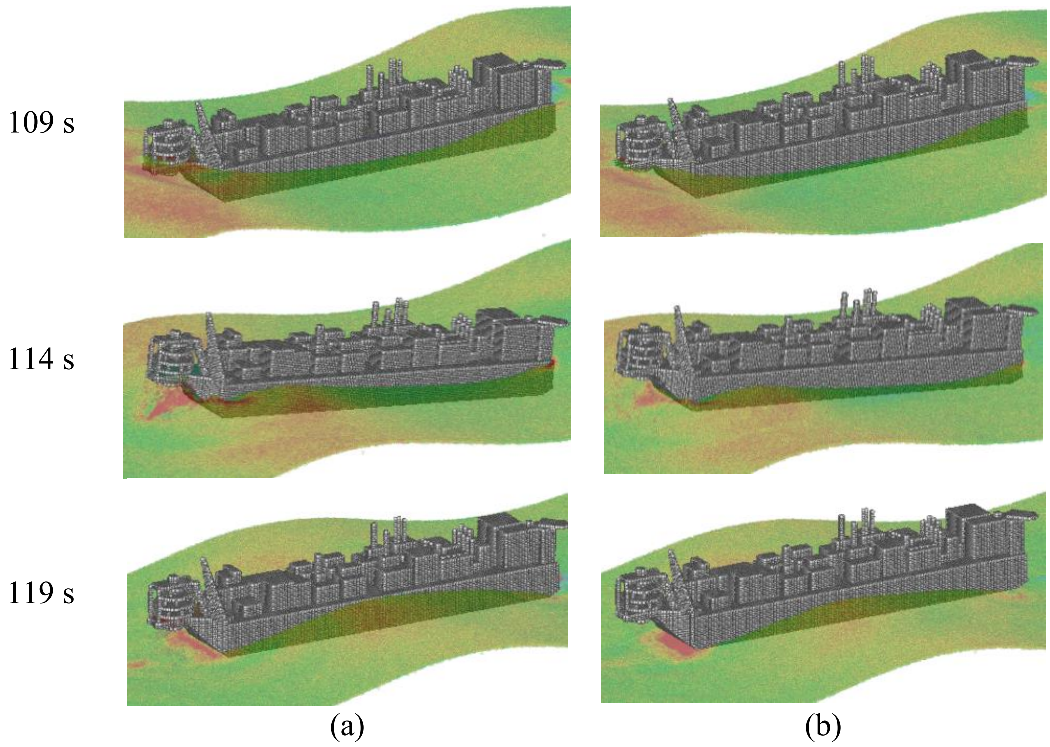


**Figure 8:** Snapshots of the particle-based simulations for the FLNG model for the maximum draught condition (a) and the minimum draught condition (b)

The maximum water levels at the bow, at the stern and at the middle section of the hull were evaluated in order to verify the occurrence of the green water phenomena. The water levels were measured in relation to the keel of the hull, in a local coordinate system. The Figure 9 shows the water level for the maximum and the minimum operational draught.

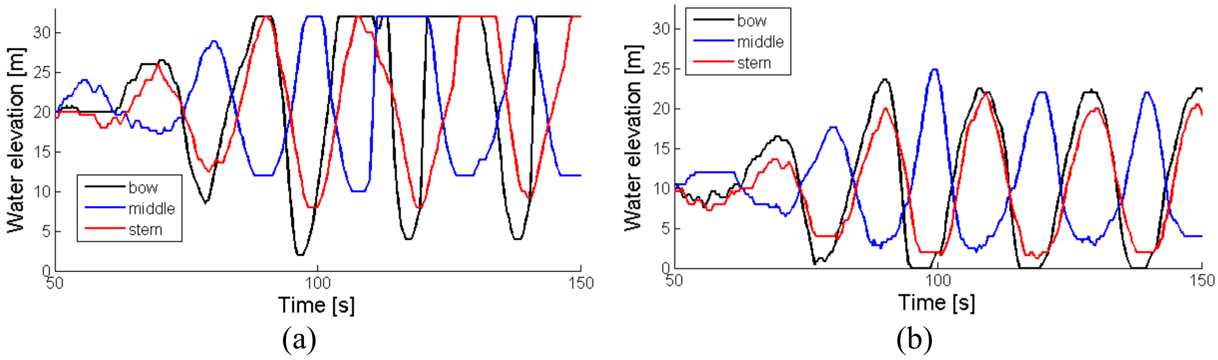


**Figure 9:** Maximum water level on the hull side for critical wave condition: Maximum draught (a) and minimum draught (b)

The FLNG system depth is approximately 33 meters. In Figure 9, when the water levels reach 33 meters, it indicates the presence of water on deck level and the occurrence of green water. The Figure 9 shows that the green water occurs only for the maximum draught condition. This behavior could also be observed at the snapshots of Figure 8, where the wave crest is very close to the deck level for the maximum operational draught condition.

## 4 CONCLUDING REMARKS

This paper presents the recent developments of a particle-based numerical offshore tank for the study of the green water phenomenon through three section: The first section shows the validation and convergence study based on a fixed FPSO model. The results show that the use of higher resolution models is more critical when accuracy is required for the regions where the level of embarking water is relatively low. The second section shows the importance of the simulation using floating models that take into account the relative motion between the floating body and the wave surface. A very high resolution floating model with 100 million particles was used to evaluate the performance of the distributed memory parallel processing. Finally, the third section shows an application of the numerical offshore tank. The recent achievements on the simulation of real scale high resolution models, with up to 100 million particles using the distributed memory architecture, provided speedup and scalability required for the application to practical engineering problems involving fluid-structure interaction problems with complex geometry and free surface.

## ACKNOWLEDGEMENTS

The authors thank PETROBRAS for the financial support during the development of the particle-based numerical simulation system in Numerical Offshore Tank (TPN-USP) and to INPEX for the financial support on the study of the green water phenomena.

## REFERENCES

[1] S. Koshizuka, H. Tamako., and Y. Oka, "A Particle Method for Incompressible Viscous Flow with Fluid Fragmentation," *Journal of Computational Fluid Dynamics*, pp. 29-46, 1995.

[2] S. Koshizuka and Y. Oka, "Moving particles semi-impliciti method for fragmentation of

incompressible fluid," *Nuclear Science and Engineering*, vol. 123, pp. 421-434, 1996.

[3] Kazuya Shibata and Seiichi Koshizuka, "Numerical Analysis of Shipping Water Impact on a Deck Using a Particle Method," *Ocean Engineering*, vol. 34, pp. 585–593, 2007.

[4] Kazuya Shibata, Seiichi Koshizuka, and Katsuji Tanizawa, "Three-dimensional Numerical Analysis of Shipping Water Onto a Moving Ship Using a Particle Method," *Journal of Marine Science and Technology*, pp. 214-227, 2009.

[5] Kazuya Shibata, Seiichi Koshizuka, Mikio Sakai, and Katsuji Tanizawa, "Lagrangian Simulations of Ship-Wave Interactions in Rough Seas," *Ocean Engineering*, 2012.

[6] Cezar Augusto Bellezi, Liang-Yee Cheng, and Kazuo Nishimoto, "Particle Based Numerical Analisys of Green Water on FPSO Deck," in *32nd International Conference on Ocean, Offshore and Arctic Engineering - OMAE 2013*, Nantes, France, 2013a.

[7] Hyun-Ho Lee, Ho-Jeong Lim, and Shin Hyung Rhee, "Experimental Investigation of Green Water on Deck for a CFD Validation Database," *Ocean Engineering*, vol. 42, pp. p. 47-60, 2012.

[8] Cezar Augusto Bellezi, Liang-Yee Cheng, and Kazuo Nishimoto, "A numerical study of the effects of bow shape on green water phenomenon," in *23rd International Conference on Ocean and Polar Engineering - ISOPE 2013*, Anchorage, 2013b.

[9] D. T. Fernandes, Implementação de Framework Computacional de Paralelização Híbrida do Moving Particles Semi-Implicit Method para Modelagem de Fluídos Incompressíveis, Ph.D. thesis, Polytechnic School of Engineering of University of São Paulo, São Paulo, Brazil, 2013.

[10] Yuxin Zhang, Xuyang Wang, Zhenyuan Tang, and Decheng Wan, Numerical Simulation of Green Water Incidents Based on Parallel MPS Method, 2013.

[11] B.-H. Lee, J.-C. Park, and M.H. Kim, "Two-dimensional vessel-motion/liquid-sloshing interactions and impact loadings by using a particle method," in *Proceedings of the ASME 2010 29th International Conference on Ocean, Offshore and Arctic Engineering - OMAE2010*, Shanghai, China, June 2010.

[12] M. Sueyoshi and S. Naito, "Aplication of MPS for Violent Free Surface Problems on Marine Engineering," Tokyo, Graduate school of Engineering 2002a.

[13] M. Sueyoshi and S. Naito, "A Numerical Study of Very Large Motion of Floating Body by Particle Method," in *Asia and Paciffic Maritime Congress*, Kobe, Japan, 2002b.

[14] Márcio Michiharu Tsukamoto, Liang-Yee Cheng, and Kazuo Nishimoto, "Numerical study of the motions in shallow water waves of floating bodies elastically linked to the bottom," in *28th International Conference on Ocean, Offshore and Arctic Engineering - OMAE 2009*, Honolulu, USA, 2009.

[15] Márcio Michiharu Tsukamoto, Liang-Yee Cheng, and Kazuo Nishimoto, "Numerical study of the effectiveness of a moving sloshing supression device," in *29th International Conference on Ocean, Offshore and Arctic Engineering - OMAE 2010*, Shanghai, China, 2010.